J Low Temp Phys (2008) 153: 140–161
DOI 10.1007/s10909-008-9844-0

Gradual Eddy-Wave Crossover in Superfluid Turbulence

Victor S. L'vov · Sergey V. Nazarenko · Oleksii Rudenko

Received: 8 July 2008 / Accepted: 5 August 2008 / Published online: 10 October 2008

Abstract We revise the theory of superfluid turbulence near the absolute zero of temperature and suggest a differential approximation model for the energy fluxes in the k-space, $\varepsilon_{\rm HD}(k)$ and $\varepsilon_{\rm KW}(k)$, carried, respectively, by the collective hydrodynamic (HD) motions of quantized vortex lines and by their individual uncorrelated motions known as Kelvin waves (KW). The model predicts energy spectra of the HD and the KW components of the system, $\mathcal{E}_{\rm HD}(k)$ and $\mathcal{E}_{\rm KW}(k)$, which experience a smooth crossover between different regimes of motion over a finite range of scales. For an experimentally relevant range of $\Lambda \equiv \ln(\ell/a)$ (ℓ is the mean intervortex separation and a is the vortex core radius) between 10 and 15 the total energy flux $\varepsilon = \varepsilon_{\rm HD}(k) + \varepsilon_{\rm KW}(k)$ and the total energy spectrum $\mathcal{E}(k) = \mathcal{E}_{\rm HD}(k) + \mathcal{E}_{\rm KW}(k)$ are dominated by the HD motions for $k < 2/\ell$. In this region $\mathcal{E}(k)$ follows the HD spectrum with constant energy flux $\varepsilon \simeq \varepsilon_{\rm HD}$ =const.: $\mathcal{E}(k) \propto k^{-5/3}$ for smaller k and tends to equipartition of the HD energy $\mathcal{E}(k) \propto k^2$ for larger k. This bottleneck accumulation of the energy spectrum is milder than the one predicted before in (L'vov et al. in Phys. Rev. B 76:024520, 2007) based on a model with sharp HD-KW transition. For $\Lambda = 15$, it results in a prediction for the effective viscosity $\nu' \simeq 0.004\kappa$ (κ is the circulation quantum) which is in a reasonable agreement

V.S. L'vov (✉) · O. Rudenko
Department of Chemical Physics, The Weizmann Institute of Science, Rehovot 76100, Israel
e-mail: Victor.Lvov@weizmann.ac.il

O. Rudenko
e-mail: oleksii.rudenko@weizmann.ac.il

V.S. L'vov
Department of Theoretical Physics, Institute for Magnetism, Ukraine National Acad. of Sci., Kiev, Ukraine

S.V. Nazarenko
Mathematics Institute, University of Warwick, Coventry, CV4 7AL, UK
e-mail: snazar@maths.warwick.ac.uk

with its experimental value in ^{4}He low-temperature experiment $\approx 0.003\kappa$ (Walmsley et al. in Phys. Rev. Lett. 99:265302, 2007). For $k > 2/\ell$, the energy spectrum is dominated by the KW component: almost flux-less KW component close to the thermodynamic equilibrium, $\mathcal{E} \approx \mathcal{E}_{\rm KW} \approx$ const at smaller k and the KW cascade spectrum $\mathcal{E}(k) \to \mathcal{E}_{\rm KW}(k) \propto k^{-7/5}$ at larger k.

Keywords Quantum turbulence · Liquid helium · Kelvin waves · Eddy-wave crossover · Bottleneck

1 Introduction

Liquid ^{4}He and ^{3}He at low temperatures can be viewed as a superfluid with almost no normal fluid present. Turbulence is a very common state for such superfluids. For this particular application and in general, turbulence comprises one of the most interesting subjects in physics with exciting recent developments; see, e.g. [3–17]. Superfluid turbulence consists of a tangle of quantized vortex lines [3–6, 18, 19]. How is the superfluid turbulence related to the usual hydrodynamical turbulence? On the one hand, at the scales greater than the mean distance between the inter-vortex separation distance one can expect the vortex discreteness to be unimportant and, therefore, the superfluid and the hydrodynamical turbulence should have similar properties at these scales. This can be true, of course, if the superfluid vortex tangle is not completely random but is polarized and organized into vortex bundles which, at large scales, form similar motions as would continuous hydrodynamic eddies. In turn, such a vortex polarization can be either introduced by an external forcing (yet to be understood how), or it can occur due to a (yet to be found) self-organization mechanism. On the other hand, since there is no viscosity, the superfluid energy would cascade downscale without loss until it reaches to the small scales where the quantum discreteness of vorticity is important. It is believed that at this point the Kolmogorov-type (K41) eddy dominated cascade is replaced by a cascade due to nonlinearly interacting Kelvin waves. Kelvin wave cascade takes energy further downscale where it can be radiated away by phonons.

Although the overall picture of superfluid turbulence described above seems quite reasonable, some important details of this picture are yet to be established. A particularly interesting question is about the structure of the crossover between the eddy dominated and the wave dominated regions of the spectrum. As it was pointed out in our recent paper [1], the nonlinear transfer mechanisms among weakly nonlinear Kelvin waves on discrete vortex lines is less efficient than the energy transfers due to the strongly nonlinear eddy-eddy interactions in continuous fluids. This results is an energy cascade stagnation at the crossover from the collective eddy dominated to the single-vortex wave dominated scales. The main message of paper [1] is that such a *bottleneck* phenomenon is robust and common for all the situations where the energy cascades experience a continuous-to-discrete transition, and the details of particular mechanism of this transition are secondary. Indeed, most discrete physical

processes are less efficient than their continuous counterparts.[1] On the other hand, particular mechanisms of the continuous-to-discrete transition can obviously lead to different strengths of the bottleneck. A quantitative measure of the bottleneck is the rms vorticity value, because this is a quantity which enters into the definition of the effective viscosity, the latter being experimentally observable via measuring decay of the vortex line density [3, 9] (see below).

Paper [1] considers the bottleneck mechanism under the simplest assumption that a sharp transition from the K41 eddy dominated cascade to the Kelvin wave weak turbulence occurs at the mean inter-vortex separation scale ℓ. In this case, the vortex line reconnections provide a mechanism to transfer the energy from the eddy to the wave motions, but their role for the energy cascade itself was neglected (even though it was noted that the bottleneck strength can be affected if this role was taken into account). On the other hand, paper [20] considered another extreme when the reconnections are the key process for the crossover cascade, and it was suggested that this process goes through three different stages in a rather narrow range of scales of width Λ—bundle-dominated, the nearest neighbor and self reconnections. In spite of this rather unrealistic construction, the end result was still a bottleneck and reduction of the effective viscosity, though by a smaller factor than predicted in [1], Λ instead of Λ^5.

In the present paper we neglect the role of the reconnections for the cascade process because, as we argued in [1], the reconnections are strongly inhibited within the polarized vortex bundles, and their occurrence is limited to the edges of these bundles. Since the volume in between of the bundles is small compared to the volume inside of these bundles, it seems natural to assume that the main contribution to the cascade will be due to nonlinear dynamics of non-reconnecting vortex lines inside the vortex bundles, even though it is still possible that the reconnections can adjust the strength of the bottleneck, particularly if the K41 range is not too large and the turbulence polarization is reduced.[2] The final answer about the role of reconnections should, of course, be sought in the experimental and the numerical data. In the present paper, we extend the analysis of [1] by taking into account the fact that Kelvin waves can be generated and play a role in the energy cascade at the scales greater than ℓ, and that the transition from the eddy to the wave motions occurs over an extended range of scales rather than sharply.

[1] It is interesting to make comparison with turbulence of weakly nonlinear waves where the main energy transfer mechanism is due to wavenumber and frequency resonances. In bounded volumes the set of wave modes is discrete and there are much less resonances between them than in the continuous case, so the energy cascades between scales are significantly suppressed.

[2] We emphasize here that we mean small contribution of the reconnections to the *cascade* (i.e. to the transfer of energy from one scale to another) and not a role of the reconnections in transferring the energy from the eddies to the waves. The latter role of the reconnections may be quite significant, although its relative importance with respect to non-reconnection type wave generation by non-stationary eddies is yet to be understood. As will be seen below, we model both types of these eddy-to-wave transfers as local in scale processes via term $F(k)$ in (18).

2 Bottleneck Scenario with Sharp Crossovers

2.1 Dimensional- and Velocity-Crossover Scales

When the "bottleneck" effect was first described in [1], it was assumed that the crossover from the eddy motions to the wave motions happens sharply at the scale $\simeq \ell$, i.e. at the mean intervortex distance or, in the k-space, at $k \simeq k_{\rm dim}$, where

$$k_{\rm dim}\ell \simeq 1. \tag{1a}$$

Subscript dim reminds that estimate (1a) follows from the simplest possible dimensional reasoning. Besides, it roughly means that at the scales larger than ℓ the vortex lines must be polarized and must form bundles which would correspond, in a coarse-grained sense, to the usual hydrodynamic eddies, while for $k > k_{\rm dim}$ the vortex motions can be viewed as oscillations independently happening on the individual vortex lines, i.e. as 1D Kelvin waves. On the other hand, it was also remarked in [1] that the self-induced motion of the vortex line can get faster than its motion due to the collective interaction with the other vortices in the bundle already at the scales $k > k_{\rm vel}$, where

$$k_{\rm vel}\ell \simeq \sqrt{2/\Lambda}. \tag{1b}$$

Subscript vel reminds that estimate (1b) follows from comparison of the self-induced velocity with cross-velocity induced at a given vortex line by nearby ℓ-distant vortex line. Notice, that the critical wavenumber given by (1b) plays an important role in the vortex-reconnection scenario presumed by Kozik and Svistunov [20]. A detailed discussion of the role of this characteristic scale in our model is given below in Appendix A.2.

Thus, Kelvin waves can be expected to be present in some form already in the wave-vector range from $k_{\rm vel}$ to $k_{\rm dim}$ where they would coexist with the collective/eddy motions. It was argued, however, that due to their oscillatory character the waves would contribute much less into the cumulative motion of the vortex bundles in this scale range.

Before going into details what occurs in the transition range

$$k_{\rm vel} < k < k_{\rm dim}, \tag{1c}$$

it is worthwhile to reconsider some aspects of the problem under the simplest assumption that only one crossover scale is relevant. This is the subject of the current section.

2.2 Bottleneck Predictions in the Presence of Dimensional- and Velocity-Crossovers

Here we reconsider the simplest scenarios of the eddy-wave transition with a sharp crossover with the only difference from [1] that the crossover scale k_* is not necessarily at $k_{\rm dim} \simeq 1/\ell$ but lies somewhere in the range (1c). To this end, we remind the Kozik–Svistunov (KS) spectrum of Kelvin waves [21], in the form suggested in [1]:

$$\mathcal{E}_{\rm KW}(k) \simeq \Lambda\left(\kappa^7\varepsilon/\ell^8\right)^{1/5}|k|^{-7/5}. \tag{2}$$

Here $\mathcal{E}_{\rm KW}(k)$ is the one-dimensional (in the $\boldsymbol{k}$-space) energy density of Kelvin waves, normalized such that $E_{\rm KW} = \int \mathcal{E}_{\rm KW}(k)\,dk$ is their total energy in the unit volume, κ is the quantum circulation and ε is the energy flux over scales. Parameters ε and ℓ are mutually dependent, and their relation follows from the expression for the rms vorticity in the system of quantum filaments, $\sqrt{\langle|\omega|^2\rangle} \simeq \kappa\ell^{-2}$. The mean-square vorticity can be found for well developed turbulence when $\langle|\omega|^2\rangle$ is dominated by the classical-quantum crossover scale k_*. In the present case

$$\langle|\omega|\rangle^2 = 2\int^{k_*} k^2\mathcal{E}_{\rm HD}(k)\,dk \simeq \int^{k_*} k^2\mathcal{E}^{\rm TE}_{\rm HD}(k)\,dk \simeq k_*^3\,\mathcal{E}_{\rm KW}(k_*). \tag{3}$$

Here the integration starts from the energy containing scale, and $\mathcal{E}^{\rm TE}_{\rm HD}$ is the thermalized part of the HD spectrum, $\mathcal{E}^{\rm TE}_{\rm HD}(k) \sim k^2$ [1]. Both integrals are dominated by the upper limit k_*, where $\mathcal{E}^{\rm TE}_{\rm HD}(k_*) \simeq \mathcal{E}_{\rm KW}(k_*)$. In (3) we omitted the contribution of Kelvin waves to the total vorticity and, consequently, to the vortex length density L. It means that the value of L used in the definition of $\ell \equiv L^{-1/2}$ is a "smoothed" vortex length from which the Kelvin-wave contributions at scales less than ℓ are removed.

Combining together (2) and (3), one gets

$$\varepsilon \simeq \kappa^3 \big/ \Lambda^5\ell^{12}k_*^8. \tag{4}$$

Factor 2 in (3) follows from a summation over the vector indices under the assumption of isotropy of the turbulent spectra. Equation (4) corresponds to the effective viscosity

$$\nu' = \frac{\varepsilon\ell^4}{\kappa^2} \simeq \kappa \big/ \Lambda^5(k_*\ell)^8. \tag{5}$$

Under the simplest assumption $k_* \simeq k_{\rm dim} \simeq 1/\ell$, one gets the value reported in [1]: $\nu' \simeq \kappa/\Lambda^5$. For the sharp crossover at the velocity-crossover scale $k_{\rm vel} \simeq 1/(\ell\sqrt{\Lambda})$, where the self-induced velocity is of the order of the cross-induced velocity (see below), one gets $\nu' \simeq \kappa/\Lambda$. As we have argued before, we expect the true value of the crossover scale to be somewhere in the region (1c). Thus, one expects that the true value of the bottleneck and corresponding ν' is somewhere in between of the two extreme values

$$\kappa\Lambda^{-5} < \nu' < \kappa\Lambda^{-1}. \tag{6}$$

Note that formally the value $\nu' \simeq \kappa\Lambda^{-1}$ is the same as the one predicted by the Kozik and Svistunov approach based on the reconnections [20].

2.3 Bottleneck at Sharp Amplitude-Crossover

Let us now check the consistency of the assumed in the previous section sharp crossover at some k_* in the interval (1c). For this, let us evaluate the amplitude $h(k_*)$ of the Kelvin waves at this scale. Obviously, for consistency this amplitude must remain less than the intervortex separation $h(k_*) < \ell$. This allows one to introduce the *amplitude-crossover scale* $k_{\rm amp}$, at which

$$h(k_{\rm amp}) \simeq \ell. \tag{7a}$$

The estimate for $h(k)$ can be obtained from the Hamiltonian of Kelvin waves a in the so-called local-induction approximation (see, e.g., (5b) in our Ref. [1]):

$$h(k) \simeq \sqrt{\mathcal{E}_{\mathrm{KW}}(k) \big/ \Lambda \kappa^2 k^3}. \tag{7b}$$

Substituting here $\mathcal{E}_{\mathrm{KW}}(k)$ from (2) and using (4) and (7a) one gets an estimate

$$k_{\mathrm{amp}} \ell \simeq \sqrt[6]{2 \big/ \Lambda}, \tag{7c}$$

which is inside of the region (6). The subscript amp reminds that estimate (7c) follows from comparison of the wave amplitude with the intervortex distance. Factor 2 under the root is put by analogy with (1b) to ensure that $k_{\mathrm{vel}} < k_{\mathrm{amp}}$ for any Λ. Assuming a sharp crossover at this scale one gets from (5):

$$\nu' \simeq \kappa \Lambda^{-11/3}, \tag{8}$$

which is, as expected, within the range (6).

So, in order for the wave amplitude to be less than the intervortex distance, the inequality $k > k_{\mathrm{amp}}$ must hold. The problem is to clarify what happens in the interval

$$k_{\mathrm{vel}} < k < k_{\mathrm{amp}}, \tag{9}$$

where the formally computed [with the Kelvin-wave spectrum (2)] wave amplitude h exceeds the intervortex distance ℓ, which cannot physically happen. For example, at the scale k_{vel} one gets from (7b): $h \simeq \Lambda \ell \gg \ell$. On the other hand, the motions with $k > k_{\mathrm{vel}}$ cannot be considered as pure collective, because the cross-velocity (which is the influence of the motion of one vortex line in the place of another one) is smaller than the self-induced velocity (for more detailed discussion of this question, see Appendix A.2).

Our scenario is that in the interval (9) the growth of the wave amplitude on a particular vortex line would be arrested by the adjacent vortex lines in the bundle which would "get in the way". Speculations of similar type of Kozik and Svistunov [20] lead them to a suggestion that the hydrodynamic and the wave turbulence ranges are separated by the range of scales where the energy cascade is dominated by the vortex line reconnections. On the other hand, it was pointed out in [1] that, because the vortex lines in turbulence must be polarized and organized in bundles, the reconnection process must be suppressed and pushed to small volumes in between of the vortex bundles. Instead of a reconnection, one can expect a restriction of the wave motion of an individual vortex line when it grows in amplitude and tries to push close to the other vortex lines in the bundle. Naturally the growth of such a wave would get arrested at the amplitude when the inter-vortex energy (which grows due to shortening of the distance to the considered vortex line) becomes equal to the vortex self-energy.

This leads us to the following physical model of turbulence in the range (9). In the **x**-space, turbulence consists of vortex bundles with a fractal structure. Each vortex bundle is made of denser sub-bundles such that the mean separation of lines within the sub-bundle is $\ll \ell$ and the mean distance between the sub-bundles is $\gg \ell$. In turn, each sub-bundle consists of even denser sub-sub-bundles, etc. The density of vortex

lines within a particular sub-bundle is such that at the scale of this sub-bundle the self-energy [which can be considered as the energy of the Kelvin waves $\mathcal{E}_{\rm KW}(k)$] and inter-vortex energies [which should be associated with the hydrodynamic energy $\mathcal{E}_{\rm HD}(k)$] are balanced. This corresponds to condition in the $\boldsymbol{k}$-space,

$$\mathcal{E}_{\rm HD}(k) \simeq \mathcal{E}_{\rm KW}(k), \tag{10}$$

in the range (9). For $k > k_{\rm amp}$, Kelvin waves can propagate on an individual vortex line without approaching to (and being influenced by) the adjacent vortex lines. In the other words, the range $k > k_{\rm amp}$ is dominated by the Kelvin wave turbulence and the role of the eddy component will be clarified below.

As we see, our corrected scenario which takes into account that the eddy/wave crossover occurs over a finite range of scales predicts a bottleneck value which is in between of the values obtained by assuming sharp transitions at the scales ℓ and $\ell\sqrt{\Lambda}$, respectively.

3 Finite Crossover Range Model

The goal of this section is to relax the simplified assumption that the bottleneck happens at some sharp crossover scale and to present a minimal semi-quantitative model for the transition regimes around the characteristic scales introduced in the previous section. The first step in this direction is to revise the differential approximation for the turbulent energy cascades; this is done in the following subsection.

3.1 Differential Approximation for the Turbulent Energy Cascades

The energy spectrum $\mathcal{E}(k,t)$ of isotropic turbulence can be described by the continuity equation

$$\frac{\partial \mathcal{E}(k,t)}{\partial t} + \frac{\partial \varepsilon(k,t)}{\partial k} = 0, \tag{11a}$$

where $\varepsilon(k,t)$ is the turbulent energy flux over scales. In the stationary case, this equation simplifies to the requirement of constancy of the energy flux in the so-called inertial interval, where both energy pumping and energy dissipation can be neglected (see, e.g. textbooks [22] or [23]):

$$\varepsilon(k) = \varepsilon. \tag{11b}$$

In order to describe a stationary spectrum $\mathcal{E}(k)$ one needs to know how $\varepsilon(k)$ depends on $\mathcal{E}(k)$. In this paper we will use reasonably simple differential models which describe the energy cascades of the hydrodynamic (HD) and the Kelvin wave (KW) turbulence at least qualitatively and sometimes even semi-quantitative.

The differential equation model for HD was first proposed by Leith in 1967 [24] and was recently studied in [25]:

$$\varepsilon_{\rm HD}(k) = -\frac{1}{8}\sqrt{k^{11}\mathcal{E}_{\rm HD}(k)}\,\frac{d}{dk}\frac{\mathcal{E}_{\rm HD}(k)}{k^2}. \tag{12}$$

Here $\varepsilon_{\rm HD}(k)$ is the energy flux carried by the HD turbulence. For (12), the factor $1/8$ reproduces a numerical coefficient that reasonably fits the experimentally observed value of the Kolmogorov constant.

The generic HD spectrum with a constant energy flux was found in [25] as a solution to the equation $\varepsilon_{\rm HD}(k) = \varepsilon = \text{const}$:

$$\mathcal{E}_{\rm HD}(k) = k^2 \left[\frac{24\,\varepsilon}{11\,k^{11/2}} + \left(\frac{T}{\pi\rho} \right)^{3/2} \right]^{2/3}. \tag{13a}$$

The large k range describes a thermalized part of the spectrum with equipartition of energy characterized by an effective temperature T, namely, $T/2$ of energy per a degree of freedom, thus, $\mathcal{E}_k = Tk^2/\pi\rho$. At low k, (13a) coincides with the K41 spectrum:

$$\mathcal{E}_{\rm HD}(k) = (24/11)^{2/3}\ \varepsilon^{2/3}\, k^{-5/3}. \tag{13b}$$

For Kelvin turbulence, the differential approximation model was suggested in [26]. In a way similar to (12), we suggest here a differential approximation for the energy flux, carried by the Kelvin waves:

$$\varepsilon_{\rm KW}(k) = -\frac{5}{7} \frac{(k\ell)^8 \mathcal{E}_{\rm KW}^4(k)}{\Lambda^5 \kappa^7} \frac{d\mathcal{E}_{\rm KW}(k)}{dk}. \tag{14}$$

Note that this form is slightly less general than the one of [26] because it does not take into account conservation of the waveaction. However, it is simpler and this allows a more detailed analytical treatment.

In the stationary case, equation $\varepsilon_{\rm KW}(k) = \varepsilon = \text{const}$ has the solution

$$\mathcal{E}_{\rm KW}(k) = \left[\frac{\Lambda^5 \kappa^7}{\ell^8} \frac{\varepsilon}{k^7} + \left(\frac{T}{\pi\rho} \right)^5 \right]^{1/5}. \tag{15a}$$

This solution changes from the KS spectrum for small k,

$$\mathcal{E}_{\rm KW}(k) \simeq \Lambda \left(\kappa^7 \varepsilon / \ell^8 \right)^{1/5} k^{-7/5}, \tag{15b}$$

to the thermodynamically equilibrium solution with equipartition of energy (Rayleigh–Jeans spectrum)

$$\mathcal{E}_{\rm KW}(k) = T/\pi\rho \tag{15c}$$

for large k. The factor $-5/7$ in (14) is chosen such to reproduce in (15b) the numerical coefficient equal to unity. The actual value of this factor is still not established with a reasonable accuracy, see, e.g. [21].

When the eddy (HD) and the KW turbulence coexist, both models should work together in such a manner that for small k the HD spectrum should be recovered, while for large k only the KW spectrum should remain,

$$\mathcal{E}(k) = \begin{cases} \mathcal{E}_{\rm HD}(k), & k \ll 1/\ell, \\ \mathcal{E}_{\rm KW}(k), & k \gg 1/\ell. \end{cases} \tag{16}$$

A way to reach this physical requirement is presented in the following section.

3.2 A Unified Model for the Total Eddy-Wave Energy Flux

A relatively simple model of turbulence incorporating the two types of motions, the random eddies and the Kelvin waves, is as follows. The two types of motion coexist and interact in an extended crossover range in the following sense:

The Total Turbulent Energy Density $\mathcal{E}(k)$ and the total energy flux over scales, $\varepsilon(k)$, consist of two respective parts,

$$\mathcal{E}(k) = \mathcal{E}_{\rm HD}(k) + \mathcal{E}_{\rm KW}(k), \tag{17a}$$

$$\varepsilon(k) = \widetilde{\varepsilon}_{\rm HD}(k) + \widetilde{\varepsilon}_{\rm KW}(k), \tag{17b}$$

where energy fluxes $\widetilde{\varepsilon}_{\rm HD}(k) = \varepsilon_{\rm HD}(k) + \varepsilon_{\rm HD}^{\rm KW}$ and $\widetilde{\varepsilon}_{\rm KW}(k) = \varepsilon_{\rm KW}(k) + \varepsilon_{\rm KW}^{\rm HD}(k)$ have additional contributions $\varepsilon_{\rm HD}^{\rm KW}(k)$ and $\varepsilon_{\rm KW}^{\rm HD}(k)$ that originate from influence of KW on the HD-energy flux and vise versa.

Continuity Equations (11a) *for the Energy Densities* have to be supplemented by additional terms $\pm F(k)$, that describe energy exchange between two types of motion:

$$\frac{\partial \mathcal{E}_{\rm HD}(k,t)}{\partial t} + \frac{\partial \widetilde{\varepsilon}_{\rm HD}(k,t)}{\partial k} = -F(k,t), \tag{18a}$$

$$\frac{\partial \mathcal{E}_{\rm KW}(k,t)}{\partial t} + \frac{\partial \widetilde{\varepsilon}_{\rm KW}(k,t)}{\partial k} = F(k,t), \tag{18b}$$

Cross-Contributions to the Energy Fluxes $\varepsilon_{\rm HD}^{\rm KW}(k)$ and $\varepsilon_{\rm KW}^{\rm HD}(k)$ are modeled in the linear approximation with respect of the counterpart energies (here HD is counterpart to KW and vice versa):

$$\varepsilon_{\rm HD}^{\rm KW}(k) = \mathcal{D}_{\rm HD}\{\mathcal{E}_{\rm HD}\}\, d\,[\mathcal{E}_{\rm KW}(k)/k_*^2]/dk^2, \tag{19a}$$

$$\varepsilon_{\rm KW}^{\rm KW}(k) = \mathcal{D}_{\rm KW}\{\mathcal{E}_{\rm KW}\}\, d\,[\mathcal{E}_{\rm HD}(k)/k^2]/dk^2, \tag{19b}$$

with some wave-vector k_* which will be clarified later. The differential form of these contributions follows from a physical hypothesis that these terms should disappear (or become much smaller and can be neglected) when the counterpart subsystem is in thermodynamical equilibrium, i.e. when $\mathcal{E}_{\rm HD} \propto k^2$ and $\mathcal{E}_{\rm KW} \propto k^0 = \text{const}$. Functionals of the corresponding energies, $\mathcal{D}_{\dots}\{\dots\}$, will be modeled by dimensional reasoning exactly in the way, how (12) and (14) for the fluxes were formulated. Resulting equations can be written in the form:

$$\mathcal{D}_{\rm HD}\{\mathcal{E}_{\rm HD}\} = C_{\rm HD}\sqrt{k^{11}\mathcal{E}_{\rm HD}(k)}, \tag{20a}$$

$$\mathcal{D}_{\rm KW}\{\mathcal{E}_{\rm KW}\} = C_{\rm KW}(k\ell)\, k_*^2 \mathcal{E}_{\rm KW}^4(k)\kappa^{-7}, \tag{20b}$$

where $C_{\rm HD}$ is a dimensionless parameter and $C_{\rm KW}(k\ell)$ is a dimensionless function of $k\ell$, that will be chosen below in (23).

The energy distribution between the counterpart components depends only on k and for simplicity it is assumed to be independent of the turbulence strength,

$$\mathcal{E}_{\rm HD}(k,t) = g(k\ell)\mathcal{E}(k,t), \tag{21a}$$

$$\mathcal{E}_{\rm KW}(k,t) = [1-g(k\ell)]\mathcal{E}(k,t), \tag{21b}$$

were we introduced (only) $k\ell$-dependent blending function $g(k\ell)$ which will be explained below.

Resulting Model for the Total Energy Flux $\varepsilon(k)$ Adding the two equations (18) and using (17) yields a continuity equation of type (11a) in which $\varepsilon(k)$ is given by (17b). We see that the unknown function $F(k,t)$ disappears from the game. Together with (12), (14), (17b), (19), (20) and (21) this finally gives

$$\varepsilon(k) = -\left\{\frac{1}{8}\sqrt{k^{11}g(k\ell)\mathcal{E}(k)} + \frac{5}{7}\frac{(k\ell)^8 k_*^2[1-g(k\ell)]^4\mathcal{E}(k)^4}{\Lambda^5\kappa^7}\right\} \times \frac{d}{dk}\left\{\mathcal{E}(k)\left[\frac{g(k\ell)}{k^2} + \frac{1-g(k\ell)}{k_*^2}\right]\right\}. \tag{22}$$

In the derivation of this equation we took

$$C_{\rm HD} = -1/8, \qquad C_{\rm KW}(k\ell) = -5(k\ell)^8/7\Lambda^5. \tag{23}$$

Equation (22) contains yet unknown blending function $g(k\ell)$ which will be discussed in the next section.

3.3 Separation of the Eddy and the Wave Motions

In order to find a qualitative form of the blending function we consider a system of locally (in the vicinity of some point $\boldsymbol{r}_0$) near-parallel vortex lines, separated by mean distance ℓ and supply them by index j. Notice that in principle the same vortex line can go far away and come close to $\boldsymbol{r}_0$ several times. To avoid this problem one should assign the same vortex line a different index j if it leaves (or enters) the ball of radius $\ell\sqrt{\Lambda}$ centered at $\boldsymbol{r}_0$. Each vortex line (with vortex core radius a) produces a velocity field $\boldsymbol{v}_j(\boldsymbol{r})$, which can be found by the Biot–Savart Law (35).

The total kinetic energy $E = \frac{1}{2}\sum_{i,j}\langle \boldsymbol{v}_i \cdot \boldsymbol{v}_j\rangle$ can be divided into two parts, $E = E_1 + E_2$, where

$$E_1 \equiv \frac{1}{2}\sum_j \langle v_j^2\rangle, \qquad E_2 \equiv \frac{1}{2}\sum_{i\neq j}\langle \boldsymbol{v}_i \cdot \boldsymbol{v}_j\rangle = \sum_{i<j}\langle \boldsymbol{v}_i \cdot \boldsymbol{v}_j\rangle. \tag{24}$$

The same subdivision can be made also for the energy density in the (one-dimensional) k-space, $\mathcal{E}(k) = \mathcal{E}_1(k) + \mathcal{E}_2(k)$, with the two terms that can be found via the $\boldsymbol{k}$-Fourier components of the velocity fields $\boldsymbol{v}_j(\boldsymbol{k})$ in a way similar to (24). Now our idea is as follows: energy $\mathcal{E}_1(k)$ is defined by the shape of the individual vortex lines i.e. it is determined by the Kelvin waves, while energy $\mathcal{E}_2(k)$ depends on

correlations between the shapes of different vortices which produce collective, hydrodynamic types of motions. Therefore $\mathcal{E}_1(k)$ can be associated with the Kelvin wave energy, $\mathcal{E}_1(k) \Rightarrow \mathcal{E}_{\rm KW}(k)$, while $\mathcal{E}_1(k)$ has to be associated with the hydrodynamic energy, $\mathcal{E}_2(k) \Rightarrow \mathcal{E}_{\rm HD}(k)$. This allows one to conclude that

$$g(k\ell) = \left[1 + \mathcal{E}_1(k)/\mathcal{E}_2(k)\right]^{-1}. \tag{25}$$

The rest are technicalities presented in Appendix A, where we concluded that for practical calculations it is reasonable to use the following analytical form of the blending function $g(k\ell)$,

$$g(k\ell) = g_0\left[0.32 \ln(\Lambda + 7.5)\, k\ell\right], \tag{26a}$$

where

$$g_0(k\ell) = \left[1 + \frac{(k\ell)^2 \exp(k\ell)}{4\pi(1 + k\ell)}\right]^{-1}. \tag{26b}$$

3.3.1 *Comparison of Various Crossover Scales*

With the proposed blending function we can introduce another cross-over scale $k_{\rm en}\ell$ by comparing HD and KW energies; at $k_{\rm en}\ell$ they are equal: $g(k_{\rm en}\ell) = 1/2$. As follows from (26), $k_{\rm en}\ell$ has very weak, logarithmical dependence on Λ:

$$k_{\rm en}\ell \simeq 6.64 \big/ \ln(\Lambda + 7.5), \tag{27}$$

presented in the second column in Table 1.

First column of this table displays the velocity-crossover scales, given by (1b): $k_{\rm vel}\ell \simeq \sqrt{2/\Lambda}$, while in the column 3 one finds the amplitude crossover $k_{\rm amp}\ell$, (7c), (the scale at which the formally computed via the KS spectrum wave amplitude reaches intervortex distance). The fourth column of Table 1 displays the flux-crossover scale, $k_{\rm fl}\ell$, at which the contribution of the eddy- and Kelvin-wave turbulence to the energy flux in the k-space become equal. This scale is introduced below in Sect. 3.4.

Table 1 Comparison of the energy-, the velocity-, the amplitude- and the flux-crossover scales for typical experimental values $\Lambda = 10$ and 15 and for unrealistically large values $\Lambda = 100$ and 10^3. Values of $k_{\rm fl}$ depend on ϵ defined in a self-consistent way, as explained in Sect. 3.4.3

–	1	2	3	4	5
Λ	$k_{\rm vel}\,\ell$ eq. (1b)	$k_{\rm en}\ell$ eq. (27)	$k_{\rm amp}\,\ell$ eq. (7c)	$k_{\rm fl}\ell$ numerics	$\epsilon \times 10^3$ self-cons.
10	0.45	2.3	0.76	24.4	5.2
15	0.37	2.13	0.71	24.19	4.0
10^2	0.14	1.4	0.52	22.8	0.30
10^3	0.045	0.96	0.35	22.5	1.2×10^{-3}

Notice, that $k_{\rm en}$ is well approximated by (27) also for $\Lambda < 100$. Theoretically, $k_{\rm en} \sim k_{\rm vel} \propto 1/\sqrt{\Lambda}$ and $k_{\rm en} \ll k_{\rm amp}$ in the asymptotical limit $\Lambda \to \infty$. Nevertheless, $k_{\rm en} > k_{\rm amp}$ in the region of interest, $\Lambda < 15$. Therefore the fractal structure of the vortex lines, described in Sect. 2.3, does not show up, and this allows us to use in the actual region $10 < \Lambda < 15$ the proposed simple blending function (26).

3.4 Turbulent Energy Spectra in the Differential Approximation

3.4.1 Dimensionless Representation

Now, it remains for us to solve the ODE (22) with the blending function $g(k\ell)$ given by (26). At this point, it is reasonable to non-dimensionalize the physical quantities via introducing

$$x = k\ell, \qquad e(x) = \frac{\ell}{\kappa^2}\,\mathcal{E}(x), \qquad \epsilon = \frac{\ell^4}{\kappa^3}\,\varepsilon. \tag{28}$$

In particular, with this normalization the one-dimensional energy spectra (13) and (15b) take the form

$$e_{\rm HD}(x) = (24/11)^{2/3}\epsilon^{2/3}x^{-5/3}, \tag{29a}$$

$$e_{\rm HD}(x,T) = x^2\left[\frac{24}{11}\frac{\epsilon}{x^{11/2}} + T^{3/2}\right]^{2/3}, \tag{29b}$$

$$e_{\rm KW}(x) = \Lambda\epsilon^{1/5}x^{-7/5}, \tag{29c}$$

where T is a non-dimensional temperature. And the ODE (22) to solve [with the boundary condition $e(x) \to e_{\rm KW}(x)$ for $x \gg 1$] becomes

$$\epsilon = -\left\{\frac{1}{8}\sqrt{x^{11}g(x)e(x)} + \frac{5}{7}\,\frac{x^8x_{\rm en}^2}{\Lambda^5}\big[1-g(x)\big]^4e^4(x)\right\} \times \frac{d}{dx}\,e(x)\left[\frac{g(x)}{x^2} + \frac{1-g(x)}{x_{\rm en}^2}\right]. \tag{30}$$

Here we have made the natural choice that the crossover scale k_* between the two types of thermodynamic equilibria is $k_{\rm en}$, i.e. the scale where energies of two types of motion are the same.

3.4.2 Λ-Dependence of the Energy Spectra

An instructive solution $e(x)$ with $\Lambda = 15$ and $\epsilon = 0.004$ is shown in Fig. 1, upper panel, as a (black) solid line. One sees that this solution for $x < x_{\rm en} \simeq 2.13$ follows the thermalized HD spectrum $e_{\rm HD}(x,T)$ [given by (29b) with properly chosen T] shown as a dotted (cyan) line. An important observation is that the pseudo-thermalized part of the spectrum is very pronounced in the region $x > 0.3$ where it is very different from the K41 spectra of HD turbulence $e_{\rm HD}(x) \propto x^{-5/3}$ shown as a dashed (blue)

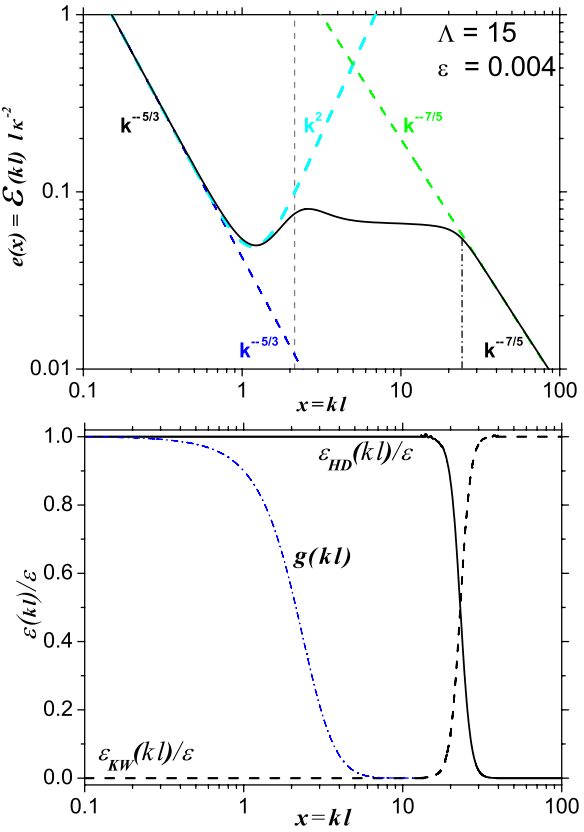

Fig. 1 (Color online) *Upper panel*: *solid* (*black*) *line* represents a typical total dimensionless energy spectrum $e(x)$ obtained by numerical solution of the ODE (30) with $\Lambda = 15$ and self-consistent value of $\epsilon = 0.004$, found in Sect. 3.4.3. *Dashed* (*blue*) *line* corresponds to the K41 energy spectrum $e_{\rm HD}(x) \propto x^{-5/3}$ with constant energy flux, *dashed* (*cyan*) *line* is general HD spectrum $e_{\rm HD}(x, T = 0.042)$, *dashed* (*green*) *line* is the KS energy spectrum of Kelvin waves $e_{\rm KW}(x) \propto x^{-7/5}$. *Vertical dashed* (*gray*) *line* shows $x_{\rm en}$. *Vertical dot-dashed* (*brown*) *line* shows position $x_{\rm fl}$, where $\epsilon_{\rm HD}(x_{\rm fl}) = \epsilon_{\rm KW}(x_{\rm fl})$. *Lower panel*: Partial energy fluxes $\epsilon_{\rm HD}(x)/\epsilon$ (*solid line*) and $\epsilon_{\rm KW}(x)/\epsilon$ (*dashed line*) obtained by numerical solution of the ODE (30) with $\Lambda = 15$ and $\epsilon = 0.004$. *Dot-dashed* (*blue*) *line* represents $g(x)$

line. For $x > x_{\rm fl}$ the solution practically coincides with the pure KS spectrum $e_{\rm KW}(x)$, (29c) shown as a dashed (green) line. Important, that the crossover scale $x_{\rm fl} \simeq 24.2$, at which the total energy flux consists of 50% of HD- and 50% of KW-fluxes, is much larger that $x_{\rm en} \simeq 2.13$, at which a half of the total energy is carried by HD and half by KW motions. To make this evident we plotted in Fig. 1, lower panel, the partial HD- and KW-energy fluxes vs. x. They become equal at $x_{\rm fl}$, which for $\Lambda = 15$ and $\epsilon = 0.004$ is around 24.2.

In the intermediate region $x_{\rm en} < x < x_{\rm fl}$ the energy consists mostly of the KW energy, while the energy flux is carried mostly by the HD motions. Explanation to this observation is simple: as follows from (30) the HD motions are more effective (in factor $\sim \Lambda^5/x^{9/2}$) in support of the energy flux then the KW turbulence. Because the main part of the energy flux is taken by the HD motions, the KW energy spectrum (and therefore the total one) is close to the flux-less KW-solution: thermodynamic equilibrium (15c), $\mathcal{E}_{\rm KW} = \text{const}$. For $x > x_{\rm fl}$, both the energy and the energy flux are carried by the KW motions. Therefore the total energy spectrum coincides with the KW cascade solution. For larger values of ϵ the flux-crossover scale goes to the smaller values of k, see Fig. 2, upper panel, remaining nevertheless larger than $k_{\rm en}$.

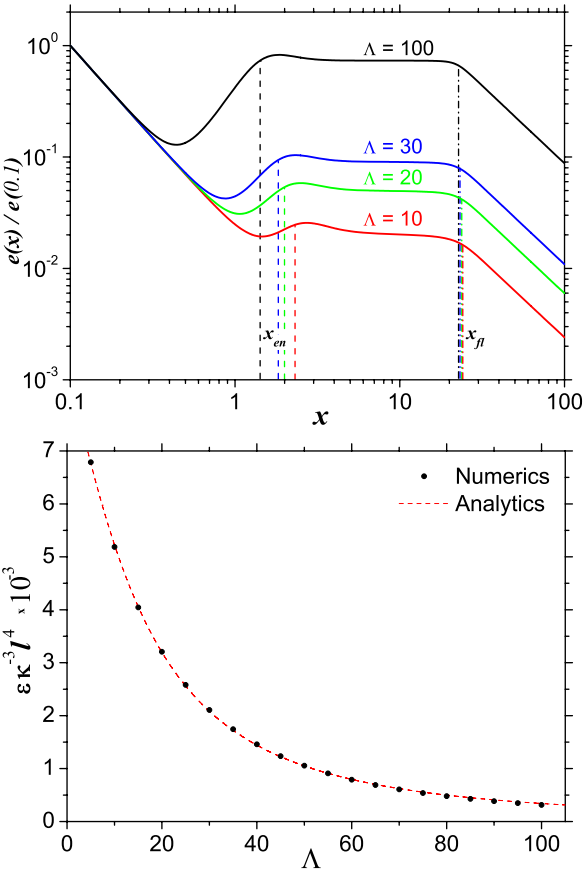

Fig. 2 (Color online) *Upper panel*: Normalized non-dimensional energies $e(x)$ at $\Lambda = 10, 20, 30$ and 100. *Vertical dashed lines* show $x_{\rm en}$. *Vertical dash-dotted lines* indicate positions of $x_{\rm fl}$ (in *red*, *green* and *blue* for corresponding ϵ). *Lower panel*: Λ-dependence of the self-consistent energy flux ϵ: (*black*) *dots*—numerical estimate as explained in Sect. 3.4.3, *dashed* (*red*) *line*—analytical approximation (32)

For smaller value of Λ qualitative behavior of $\mathcal{E}(x)$ remains the same, just different parts of the spectra (with larger values of self-consistent values of ϵ) become less pronounced.

3.4.3 Self-consistent Estimate of the Dimensionless Energy Flux

The energy spectra shown in Figs. 1 and 2 (which we obtained using our differential approximation model) are quite similar to those suggested under the assumption of a sharp crossover, see Fig. 1 in Ref. [1]. Indeed, for small k they coincide with the HD spectrum, including the bottleneck part with (almost) thermalized part $\mathcal{E} \propto k^2$, while for large k the spectrum follows the KS spectrum $\propto k^{-7/5}$. The only difference is that in the sharp-crossover case the thermalized part of the HD-spectrum is matched to the KS spectrum at some $k = k_*$, while in the differential approximation (with a smooth blending function) there is an essential intermediate region (about one decade) $k_{\rm en} < k < k_{\rm fl}$, with (almost) KW-thermalized part $\mathcal{E} = \text{const}$. This leads to an essential difference in the estimates of the vorticity $\langle\omega^2\rangle$ and as a result in the estimates of the effective viscosity ν', a parameter that can be measured (implicitly) in experiments. Indeed, in the models with the sharp crossover one estimates $\langle\omega^2\rangle$ in (3) as $k_*^3 \mathcal{E}_{\rm HD}(k_*)$

and then equates $\mathcal{E}_{\rm HD} \simeq \mathcal{E}_{\rm KW}$, because in this model the HD-energy "transforms" into the KW-energy at the position of the sharp crossover.

In the "continuous" model presented above one has to account for a wide region between $k_{\rm en}$ and $k_{\rm f1}$, where the flux is supported by the HD turbulence, while the energy is dominated by the Kelvin waves. Therefore $\langle\omega^2\rangle$ can be estimated similarly to (3) as $2\int k^2\mathcal{E}_{\rm HD}(k)dk \simeq k_{\rm en}^3\mathcal{E}_{\rm HD}(k_{\rm en})$, but now $\mathcal{E}_{\rm HD}(k_{\rm en})$ cannot be estimated based on the $-7/5$ Kozik–Svistunov spectrum because, as one sees in Fig. 2, upper panel, $\mathcal{E}_{\rm HD}$ is much lower at this point. As a result, at the same energy flux the rms vorticity $\sqrt{\langle|\omega|^2\rangle}$ appears to be essentially smaller than the one in the sharp-crossover models and the effective viscosity is larger. In our approach the rms vorticity can be found more accurately by numerical calculation of the integral in (3) with spectrum $\mathcal{E}_{\rm HD}(k) \simeq g(k\ell)\mathcal{E}(k)$, where the blending function is given by (26):

$$\langle|\omega|^2\rangle = 2\int_{k_{\rm min}}^{\infty} k^2 g(k\ell)\mathcal{E}(k)\,dk, \tag{31a}$$

where $k_{\rm min}$ is the lower cutoff of the inertial interval. Using relation $\langle|\omega|^2\rangle = \kappa^2/\ell^4$ and normalization (28) one finds from (31a) in the limit $k_{\rm min} \to 0$:

$$1 = 2\int_0^{\infty} x^2 g(x)e(x)\,dx. \tag{31b}$$

Due to the ϵ dependence of the energy spectrum e, this relation gives a self-consistent estimate of the dimensionless energy flux ϵ, which is, according to (5) and (28), nothing else but ν'/κ. Resulting dependence ϵ vs. Λ is shown in Fig. 2, lower panel, by a solid line. For convenience we approximate this dependence (in the actual interval $\Lambda < 100$) analytically:

$$\epsilon = \frac{\nu'}{\kappa} = \frac{8.65}{10^3 + 45.8\Lambda + 1.98\Lambda^2}, \tag{32}$$

shown in Fig. 2, lower panel, by a dashed line. Equation (32) reproduces the numerical dependence $\epsilon(\Lambda)$ with accuracy better than 1.5% for $\Lambda < 50$ and better than 8% for $50 < \Lambda < 100$.

Notice that the predicted value of $\epsilon = \nu'/\kappa$ for $\Lambda = 15$ is 0.004 which is quite close to the experimentally reported value $\nu' \simeq 0.003\kappa$ in ^{4}He experiments at low temperatures [2]. Relationship between our model and the experiments will be discussed below.

3.5 Decay of Quantum Turbulence with the Bottleneck Energy Accumulation

Having in mind experiments with decaying superfluid turbulence, like the ones in [2], it is important to discuss how the bottleneck energy accumulation influences the decay of energy and vorticity in time. For this, we divide the total HD energy

$$E_{\rm HD} = \int_{k_{\rm min}}^{\infty} dk\,\mathcal{E}_{\rm HD}(k) \tag{33a}$$

into a sum of two parts:

$$E_{\rm HD} = E^{\rm K41}_{\rm HD} + E^{\rm TE}_{\rm HD}, \tag{33b}$$

the energy $E^{\rm K41}_{\rm HD}$ associated with the K41 part of energy spectra $\mathcal{E}_{\rm HD} \propto k^{-5/3}$, and the energy $E^{\rm TE}_{\rm HD}$ associated with the thermodynamic equilibrium (TE) part of the spectrum $\mathcal{E}_{\rm HD} \propto k^2$. For our model:

$$E^{\rm K41}_{\rm HD} = \int_{k_{\rm min}}^{k_{\rm TE}} dk\, \mathcal{E}_{\rm HD}(k), \tag{33c}$$

$$E^{\rm TE}_{\rm HD} = \int_{k_{\rm TE}}^{\infty} dk\, \mathcal{E}_{\rm HD}(k), \tag{33d}$$

where $k_{\rm TE}$ is the crossover scale between K41 and TE parts of the energy spectra corresponding to the position where $\mathcal{E}_{\rm HD}(k)$ is minimal. For $\Lambda = 15$, $k_{\rm TE} \approx 1/\ell$, see Fig. 1, upper panel. The K41-energy, $E^{\rm K41}_{\rm HD}$, is dominated by the outer region of the k-space, $k > k_{\rm min}$, while the TE-energy is determined by effectively the largest $k \simeq k_{\rm en}$ of the HD motions (Fig. 1, upper panel). In the experiment [2], $k_{\rm min}$ is below 1 cm^{-1}, which is less than $k_{\rm en} \simeq 2/\ell$ by one or two orders of magnitude. Then, the experiment [2] allows to estimate the ratio $E^{\rm TE}_{\rm HD}/E^{\rm K41}_{\rm HD}$ in the proposed framework, and it varies from a few percents for small times to about 15–20% at the latest times of the decay measurements. For us this means that with an acceptable accuracy one can neglect the contribution of $E^{\rm TE}_{\rm HD}$ in (33b).

Moreover, even when kept in (33b), the energy $E^{\rm TE}_{\rm HD}$ has little effect on the decay rate of the $E^{\rm K41}_{\rm HD}$ energy due to a large scale separation ($k_{\rm min} \ll k_{\rm en}$). The decay rate of $E^{\rm K41}_{\rm HD}$ is determined by the energy flux $\varepsilon = -dE^{\rm K41}_{\rm HD}/dt$ at the scale of the energy pumping, i.e. at the outer scale $k = k_{\rm min}$. The flux itself is proportional to $\mathcal{E}_{\rm HD}(k)^{3/2} \sim (E^{\rm K41}_{\rm HD}/k_{\rm min})^{3/2}$. For systems with the time independent $k_{\rm min}$, as it is in [2], this gives the well known result for the late-time free-decaying HD turbulence:

$$E^{\rm K41}_{\rm HD}(t) \propto t^{-2}, \tag{34a}$$

and the time-evolution of the energy flux

$$\varepsilon(t) \propto t^{-3}. \tag{34b}$$

According to (28), $\varepsilon(t) = \epsilon\kappa^3/\ell^4(t)$ with the time-independent self-consistent dimensionless energy flux ϵ, which depends only on Λ. This gives $\ell(t) \propto t^{3/4}$. Therefore, the vortex line density must decay in the standard manner:

$$L = 1/\ell^2 \propto t^{-3/2}, \tag{34c}$$

in spite of the accumulation of energy $E^{\rm TE}_{\rm HD}$ near the crossover scale $k_{\rm en}$.

Notice, that energy $E^{\rm TE}_{\rm HD}(t)$ decays slower than $E^{\rm K41}_{\rm HD}(t) \propto t^{-2}$. Indeed, in our model the dimensionless energy $E^{\rm TE}_{\rm HD}\ell^2/\kappa^2$ (cf. (28)) is dominated by the time in-

dependent scale $x_{\rm en}$ and, hence, by itself is time independent. Therefore,

$$E^{\rm TE}_{\rm HD}(t) \propto \ell^{-2} \propto t^{-3/2}. \tag{34d}$$

One concludes that $E^{\rm TE}_{\rm HD}$ energy is "decoupled" from the decay process of $E^{\rm K41}_{\rm HD}$ energy and does not affect the decay law (34c) of the vortex line density until to the very late stage of the decay, when the intervortex distance approaches the outer scale of turbulence and the entire model fails.

4 Summary and Discussion

In this paper, we revised the theory of the bottleneck crossover from the classical K41 cascade to the Kelvin wave cascade. In its previous form, transition from the eddy to the wave cascades was assumed to occur sharply at the scale ℓ. The simple fact that the wave interactions are less efficient for the turbulent cascade than the hydrodynamic eddies immediately yields prediction for the bottleneck accumulation near the crossover scale. However, the bottleneck strength is rather sensitive to the details of the crossover region. In the present paper, we take into account that there exists a finite range where eddies and waves coexist and affect each other, making the crossover more gradual. As a result, the bottleneck in such a case is milder than in the model with the sharp crossover. To model the gradual transition range, we have employed a simplified turbulence model which is based on the differential approximation models of Leith type for the HD and KW components. Importantly, this model allows to make predictions for the realistic experimental values Λ in the range from 10 to 15, rather than making asymptotical predictions for the case $\Lambda \to \infty$. This appears to be important because, e.g., the asymptotic theory gives $k_{\rm amp} \gg k_{\rm en}$ whereas for Λ in the range from 10 to 15 we have $k_{\rm amp} < k_{\rm en}$. As a result, for the experimentally important situations there is no range with equipartition of the eddy and the wave energies given by (10). For similar reasons, the theory of crossover [20] which fits three asymptotic ranges into a single decade of scales is rather unrealistic (leaving aside the issue about the role of reconnections which we mentioned before).

One may experience some problems trying to imagine any HD components at $k\ell > 2\pi$, where the wavelength becomes smaller than the intervortex distance, and even come to an idea that $g(k\ell)$ must become zero sharply at $k\ell = 2\pi$, or generally, $k\ell \sim 1$. Our model is based on a (reasonable) hypothesis that the HD motions are identified with the coherent part of different vortex line motions. In such an approach there is no formal limitation for the value of k from above. At $k\ell > 1$ the velocity produced by k-distortion of a given vortex line in the position of another ℓ-separated line, which is the reason for correlations in their motions, decays exponentially with $k\ell$. That is why our blending function, which measures the fraction of the HD motions, decays exponentially with $k\ell$. The actual hypothesis in this place is that even when $g(k\ell) \ll 1$ the nonlinear energy flux carried by the HD motions is governed by the same equations as for the pure HD motions when $g(k\ell) = 1$.

The found value of $\epsilon = \nu'/\kappa$ for $\Lambda = 15$ is 0.004 which is quite close to the experimentally observed value $\nu'/\kappa \simeq 0.003$ in ^{4}He experiments at low temperatures

[2]. Having in mind that our model does not contain fitting parameters, optimists can consider this agreement as more than satisfactory. On the other hand, pessimists can consider any agreement with just one number as accidental. Realists may not find the detailed analysis of this model very convincing, warring about too may assumptions, and too little physical justification for the procedures being used. In particular, we should recall that the suggested model is based on a hypothesis of blending function, which was estimated without taking into the account the vectorial structure of the velocity field and, moreover, includes very important (step-like) assumption about the pair-distribution function of the vortex positions which allows one to estimate sum (41a) as integral (41b). Our feeling is that these approximations do not affect the results too much and a good agreement between the model and experimental values of ν' supports the suggested model. Notice that our model predicts not only the value of ν' but the entire energy spectrum, which consists of four parts: K41 HD energy spectrum with constant energy flux, $\mathcal{E} \propto k^{-5/3}$, a HD equilibrium $\mathcal{E} \propto k^2$, a KW equilibrium $\mathcal{E} \simeq$ const and a KW-spectrum with constant energy flux, $\mathcal{E} \propto k^{-7/5}$.

We believe that our *model* (which is not a *theory* yet), based on idea of coexistence of hydrodynamic and Kelvin-wave turbulence, is a step forward in such a difficult and challenging problem as superfluid turbulence, especially in comparison with the over-simplified *scenarios* of sharp crossover, considered in the limit $\Lambda \to \infty$. Very definite qualitative predictions obtained in this paper call for more detailed experimental and numerical study of the superfluid turbulence, which, as we believe, will support our model. When and if this happens we are planning further theoretical development of the model toward a theory of eddy-wave crossover of superfluid turbulence.

Acknowledgements We are thankful to both anonymous referees for their comprehensive analysis of our paper and detailed comments which helped us to improve the presentation of our results. V.L. is grateful to G. Volovik, M. Krusius, and V. Eltsov for involving him into a discussion of ongoing experiment on turbulence in superfluid 3He, which shed light on the bottleneck problem. This work has been partially supported by ULTI-4 (No. RITA-CT-2003-505313), Academy of Finland (Grants No. 124616, 213496, and No. 114887) and by the Transnational Access Programme at RISC-Linz, funded by the European Commission Framework 6 Programme for Integrated Infrastructures Initiatives under the project SCIEnce (Contract No. 026133).

Appendix A: Estimation of the HD-KW Blending Function

A.1 Estimation of the Velocity Field, Induced by the Vortex Distortion

To estimate the HD-KW blending function $g(k\ell)$, given by (25) we consider a vortex line slightly distorted, say in y-direction, by a sinus with a small amplitude A, running along z-axis with the k-vector k. Then $d\boldsymbol{\ell} = (0,\ Ak\cos(kz+\phi),\ 1)dz$, where ϕ is an arbitrary phase. Each line produces velocity that can be found via Bio–Savart Law:

$$\boldsymbol{v}_j(\boldsymbol{r}) = \frac{\kappa}{4\pi}\int_{-\infty}^{+\infty} \frac{d\boldsymbol{\ell}_j \times \boldsymbol{s}_j}{s_j^3}, \tag{35}$$

where $\boldsymbol{s}_j = \boldsymbol{r} - \boldsymbol{r}_j$ with $\boldsymbol{r}_j$ being the radius-vector pointing to the $\boldsymbol{\ell}_j$—the length element along the j-th vortex line and. The total mean density of the kinetic energy

per unit mass is $E = \frac{1}{2}\langle |V|^2 \rangle$, where $\boldsymbol{V}(\boldsymbol{r}) = \sum_j \boldsymbol{v}_j(\boldsymbol{r})$ is the total velocity field, and one understands $\langle \dots \rangle$ as the averaging with respect of the (random) vortex-line positions.

Using (35) we can find the resulting velocity (for simplicity) in the ZY-plane at distance R from the line. This velocity has only one component, v_x, and it is given by:

$$v_x = \frac{\kappa}{4\pi} \int_{-\infty}^{\infty} \frac{R - A\sin(kz+\phi) + Akz\cos(kz+\phi)}{\{z^2 + [R - A\sin(kz+\phi)]^2\}^{3/2}}\, dz. \tag{36}$$

Computing the contribution to the amplitude of the velocity variations proportional to the distortion amplitude A, one finds magnitude [i.e. factor in front of $\cos(kz+\phi)$] of the velocity fluctuations:

$$\delta v(R) = \frac{\kappa A}{2\pi R^2}\, kR\big\{kR\,[\,K_2(kR) - K_0(kR)\,] - K_1(kR)\big\} \tag{37a}$$

$$\Rightarrow \delta v(R) \simeq \frac{\kappa A}{2\pi R^2}\sqrt{1 + \frac{\pi}{2}kR}\,\exp(-kR), \tag{37b}$$

where K_n are modified Bessel functions of the second kind. Interesting, that a simple interpolation (37b) reproduces the exact result (37a) with an accuracy better than 2%.

Equations (37) assume that the distance R to the vortex line is large enough to be able to neglect finiteness of the core radius a. In the opposite limit, $R \ll a$, one can use an equation for the self-induced velocity, in which the core radius is hidden in the parameter $\Lambda = \ln(\ell/a)$:

$$\delta v_{\rm si} = A\Lambda k^2 \kappa/4\pi. \tag{37c}$$

Considering this equation formally as a limit for the velocity when $R \to 0$, we suggest an interpolation formula approximately valid for any R:

$$\delta v_k(R) \simeq \frac{\kappa A}{2\pi}\,\frac{\Lambda k^2 e^{-kR}}{2 + \Lambda(kR)^2}\sqrt{1 + \frac{\pi}{2}kR}, \tag{37d}$$

where subscript k reminds that this velocity is induced by vortex line, distorted by $\sin(kr)$.

A.2 Velocity Crossover Scale

A way to estimate the eddy-wave crossover scale, suggested in [20] is to compare the self-induced velocity filed with the velocity field produced by a different neighboring vortex line. To detail derivation of [20] retaining numerical factors, we consider simple geometry with two sin-disturbed parallel vortex lines separated by distance ℓ. They "start to feel" each other when $\delta v \simeq \delta v^{\rm SI}$, i.e.:

$$\delta v \simeq \delta v^{\rm SI} \quad \Leftrightarrow \quad \sqrt{4 + 2\pi\, k_{\rm vel}\ell}\, {\rm e}^{-k_{\rm vel}\ell} \simeq \Lambda(k_{\rm vel}\ell)^2. \tag{38}$$

An approximate solution to this equation (with an accuracy better than 10% for $\Lambda \geq 10$) is given by (1b). One can think that for the scales less than $k_{\rm vel}$, there is the cumulative effect and hydrodynamic-like behavior. For the scales larger than $k_{\rm vel}$

the vortices does not seem to feel each other much, and the separate vortex line behavior is important, hence the Kelvin waves. Corrections to this simplest viewpoint will be discussed below.

A.3 Estimate of the Blending Function

Having at hand an estimate of the velocity filed (37d) we can use (25) to find the blending function $g(k\ell)$.

The first step is to obtain the kinetic energy density $E_{11}(k)$ (per unit length), produced by one sin-distorted (with wave-vector k) vortex line:

$$E_{11}(k) = \frac{\rho_0}{2}\iint \big\langle \big|v_k(R,z)\big|^2 \big\rangle\, dx dy \tag{39a}$$

$$\approx \rho_0 \frac{(A\,\kappa\,\Lambda\,k)^2}{8\pi}\int_0^\infty \frac{(1+\pi\rho/2)\,e^{-2\rho}}{(2+\Lambda\rho^2)^2}\,\rho\,d\rho \tag{39b}$$

$$\approx \rho_0 \frac{\Lambda}{8\pi}(A\,\kappa\,k)^2, \quad \text{for } \Lambda \gg 1. \tag{39c}$$

Here the fluid density ρ_0 should be distinguished from the dimensionless radius $\rho = kR$, $R = \sqrt{x^2+y^2}$. In (39a) we should substitute $v_k(R,z) = v_k(R)\cos(kz+\phi)$ from (37d) integrate over (x,y)-plane orthogonal to the mean vortex line directed along z, and average $\langle\cos^2(kz+\phi)\rangle = \frac{1}{2}$ along z. Considering the integral in dimensionless polar coordinates ρ and φ after the free integration over φ, we get (39b), in which integral can be analytically taken in the limit of large Λ with the result (39c). This formula can also be obtained directly from the Kelvin-wave Hamiltonian in the so-called local-induced approximation, see e.g. (5b) in [1], where one expands $\sqrt{1+|dw(z)/dz|^2}$ over the line distortion $w(z) = A\sin(kz)$.

The second step is to find cross-kinetic energy density $E_{1j}(k,\ell_{1j})$ (per unite length), proportional to the product of the velocities produced by two sin-distorted vortex lines, separated by ℓ_{1j}.

$$E_{1j}(k,\ell_{1j}) = \rho_0\int_{-\infty}^{\infty} dx \int_{-\infty}^{\infty} dy \big\langle \big|v_k(R_1,z)v_k(R_2,z)\big|\big\rangle$$

$$= \frac{\rho_0}{2}\left(\frac{\kappa A \Lambda k}{\pi}\right)^2 \int_0^\infty \delta\widetilde{x}\int_{-\infty}^{\widetilde{\ell}_{1j}/2} \delta\widetilde{y}\, F(\rho_1)F(\rho_2)\, e^{-\rho_+}, \tag{40a}$$

$$F(\rho) = \frac{\sqrt{1+\pi\rho/2}}{2+\Lambda\rho^2}, \quad \rho_+ = \rho_1+\rho_2. \tag{40b}$$

Here $\widetilde{x} = k\,x$, $\widetilde{y} = k\,y$, $\widetilde{\ell}_{1j} = k\ell_{1j}$, $\rho_1 = k\sqrt{x^2+y^2}$ and $\rho_2 = k\sqrt{x^2+(y-\ell_{1j})^2}$. The change in the limits of integration is due to the (average) symmetry of the integrand relative to the plane $y = \ell_{1j}/2$. The main contribution to the integral comes from the region with $\widetilde{x} < \widetilde{\ell}_{1j}$, which allows to simplify the integrand replacing

$\rho_2 \Rightarrow \widetilde{\ell}_{1j} - \widetilde{y} + \widetilde{x}^2/(2\,\ell_{1j})$. This clarifies the leading dependence $E_{1j}(k, \ell_{1j})$ on ℓ_{1j} as

$$E_{1j}(k, \ell_{1j}) \propto \exp(-k\,\ell_{1j}). \tag{40c}$$

Algebraic improvement of this estimate cane be obtained by neglecting the (x, y)-dependence of $F(\rho_2)$ in (40a). This procedure can be justified asymptotically for $k\ell_{1j} \gg 1$. The resulting dependence $E_{1j}(k, \ell_{1j}) \propto F(k\ell_{1j}) \exp(-k\,\ell_{1j})$ approximates the integral (40a) with an accuracy of 10% for $k\,\ell_{1j} > 2$. For smaller $k\ell_{1j}$ one has to account for ℓ_{1j} dependence of the remained integral $\int_{-\infty}^{\ell_{1j}/2} \ldots dy \simeq (c_1/\Lambda)\ln(k\ell_{1j} + c_2)$ with c_1 and c_2 weakly dependent on Λ. As a result we approximate (with accuracy about 25%) the $k\ell_{1j}$ dependence of the energy E_{1j} as follows:

$$E_{1j}(k, \ell_{1j}) \approx \rho_0 \frac{\Lambda}{8\pi}(A\,\kappa\,k)^2\, c_1 \ln(k\ell_{1j} + c_2) \frac{\sqrt{1 + \pi k\ell_{1j}/2}}{2 + \Lambda(k\ell_{1j})^2} \exp(-k\ell_{1j}). \tag{40d}$$

In typical experiments with superfluid ^{3}He and ^{4}He the value of Λ varies from 10 to 15. Therefore we present here parameters $c_1 \approx 1.37$, $c_2 \approx 1.25$ for $\Lambda = 10$ and $c_1 \approx 1.54$, $c_2 \approx 1.22$ for $\Lambda = 15$.

The third step is to find the relative total cross-energy of all $j \neq 1$ pairs

$$R(k\ell) = \sum_{j\neq 1} \frac{E_{1j}(k, \ell_{1j})}{E_{11}(k)} \tag{41a}$$

$$\simeq \frac{4\pi}{(k\ell)^2} \int_{\ell_0}^{\infty} d\ell_{1j}\, \ell_{1j}\, \frac{E_{1j}(k, \ell_{1j})}{E_{11}(k)}, \tag{41b}$$

which is estimated in (41b) in continuous approximation assuming that j-lines are randomly distributed around line $i = 1$ with mean density $1/\ell^2$ for ℓ_{1j} exceeding, value ℓ. Generally speaking, the integral (41b) should contain probability function of vortex separations $\mathcal{P}(\ell_{ij})$. Having no reasonable model for it, we choose a simple step function $\mathcal{P}(x) = 0$ for $x > 1$.

Blending function $g(k\ell)$, defined by (25), is related to the ratio (41) as follows:

$$g(k\ell) = R(k\ell)\big/[1 + R(k\ell)], \tag{42}$$

Taking oversimplified representation (40c) of integral (40a) one computes $g_0(k\ell)$, see (26b):

$$g_0(k\ell) = \left[1 + \frac{(k\ell)^2 \exp(k\ell)}{4\pi(1 + k\ell)}\right]^{-1}. \tag{43}$$

Comparing Λ-independent function $g_0(k\ell)$ with $g_{\text{num}}(k\ell)$, which depends also on Λ, we have improved its analytical representation by introducing Λ-dependent rescaling of the argument, see (26a):

$$g(k\ell) = g_0[0.32\ln(\Lambda + 7.5)k\ell]. \tag{44}$$

The resulting function $g(k\ell)$ gives a very reasonable approximation to the results of "exact" numerical calculation of $g_{\rm num}(k\ell)$. Therefore in practical calculations we will use analytical form (26) of the blending function $g(k\ell)$.

References

1. V.S. L'vov, S.V. Nazarenko, O. Rudenko, Phys. Rev. B **76**, 024520 (2007)
2. P.M. Walmsley, A.I. Golov, H.E. Hall, A.A. Levchenko, W.F. Vinen, Phys. Rev. Lett. **99**, 265302 (2007)
3. W.F. Vinen, J.J. Niemela, J. Low Temp. Phys. **128**, 167 (2002)
4. W.F. Vinen, Phil. Trans. R. Soc. A **366**(1877), 2925–2933 (2008). doi:10.1098/rsta.2008.0084
5. M. Tsubota, arXiv:0806.2737 (2008)
6. V.B. Eltsov, R. de Graaf, R. Hanninen, M. Krusius, R.E. Solntsev, V.S. L'vov, A.I. Golov, P.M. Walmsley, in *Progress in Low Temperature Physics*, vol. 16, ed. by M. Tsubota (Elsevier, Amsterdam, 2008), in press; also arXiv:0803.3225
7. S.N. Fisher, A.J. Hale, A.M. Guénault, G.R. Pickett, Phys. Rev. Lett. **86**, 244 (2001)
8. T. Araki, M. Tsubota, S.K. Nemirovskii, Phys. Rev. Lett. **89**, 145301 (2002)
9. S.R. Stalp, J.J. Niemela, W.F. Vinen, R.J. Donnelly, Phys. Fluids **14**, 1377 (2002)
10. R. Hänninen, R. Blaauwgeers, V.B. Eltsov, A.P. Finne, M. Krusius, E.V. Thuneberg, G.E. Volovik, Phys. Rev. Lett. **90**, 225301 (2003)
11. A.P. Finne, T. Araki, R. Blaauwgeers, V.B. Eltsov, N.B. Kopnin, M. Krusius, L. Skrbek, M. Tsubota, G.E. Volovik, Nature **424**, 1022 (2003)
12. W.F. Vinen, M. Tsubota, A. Mitani, Phys. Rev. Lett. **91**, 135301 (2003)
13. D.I. Bradley, D.O. Clubb, S.N. Fisher, A.M. Guénault, R.P. Haley, C.J. Matthews, G.R. Pickett, V. Tsepelin, K. Zaki, Phys. Rev. Lett. **95**, 035302 (2005)
14. V.B. Eltsov, A.P. Finne, R. Hänninen, J. Kopu, M. Krusius, M. Tsubota, E.V. Thuneberg, Phys. Rev. Lett. **96**, 215302 (2006)
15. D.I. Bradley, D.O. Clubb, S.N. Fisher, A.M. Guénault, R.P. Haley, C.J. Matthews, G.R. Pickett, V. Tsepelin, K. Zaki, Phys. Rev. Lett. **96**, 035301 (2006)
16. V.B. Eltsov, A.I. Golov, R. de Graaf, R. Hänninen, M. Krusius, V.S. L'vov, R.E. Solntsev, Phys. Rev. Lett. **99**, 265301 (2007)
17. P.-E. Roche, C.F. Barenghi, Euro Phys. Lett. **81**, 36002 (2008)
18. R.J. Donnelly, *Quantized Vortices in He II* (Cambridge University Press, Cambridge, 1991)
19. C.F. Barenghi et al. (eds.), *Quantized Vortex Dynamics and Superfluid Turbulence*. Lecture Notes in Physics, vol. 571 (Springer, Berlin, 2001)
20. E.V. Kozik, B.V. Svistunov, Phys. Rev. B **77**, 060502(R) (2008)
21. E.V. Kozik, B.V. Svistunov, Phys. Rev. Lett. **92**, 035301 (2004)
22. L.D. Landau, E.M. Lifshitz, *Course of Theoretical Physics: Fluid Mechanics* (Pergamon, New York, 1987)
23. U. Frish, *Turbulence: The Legacy of A.N. Kolmogorov* (Cambridge University Press, Cambridge, 1995)
24. C. Leith, Phys. Fluids **10**, 1409 (1967)
25. C. Connaughton, S. Nazarenko, Phys. Rev. Lett. **92**, 044501 (2004)
26. S. Nazarenko, JETP Lett. **84**, 585 (2006)